Protist, Vol. 165, 93–111, January 2014
http://www.elsevier.de/protis
Published online date 1 December 2013

Protist

ORIGINAL PAPER

The Chaos Prevails: Molecular Phylogeny of the Haptoria (Ciliophora, Litostomatea)

Peter Vďačný[a,1], Hans-Werner Breiner[b], Varvara Yashchenko[b,c], Micah Dunthorn[b], Thorsten Stoeck[b], and Wilhelm Foissner[c]

[a]Department of Zoology, Comenius University, Mlynská dolina B-1, SK-84215 Bratislava, Slovakia
[b]Department of Ecology, University of Kaiserslautern, Erwin-Schroedinger-Strasse 14, D-67663, Germany
[c]Department of Organismal Biology, University of Salzburg, Hellbrunnerstrasse 34, A-5020 Salzburg, Austria

Submitted June 20, 2013; Accepted November 16, 2013
Monitoring Editor: David Moreira

The Haptoria are free-living predatory ciliates living in terrestrial and aquatic habitats all around the world. They belong to a highly diverse class, Litostomatea, whose morphological and molecular classifications harmonize poorly since both approaches produce rather different frameworks. In the present study, we analyzed the genealogy of the litostomateans, including eight new haptorian 18S rRNA gene sequences. Apart from traditional tree-building methods, we also applied phylogenetic networks, split spectrum analysis and quartet likelihood mapping to assess the information content of alignments. These analyses show that: (1) there are several strongly supported monophyletic litostomatean lineages — Rhynchostomatia, Trichostomatia, Haptorida, Lacrymariida, Pleurostomatida, and Didiniida; (2) the Rhynchostomatia are the best candidates for a basal litostomatean group; (3) sister relationship of the Trichostomatia and Haptoria is very likely, which well corroborates the traditional morphology-based classifications; (4) molecular phylogeny of the order Spathidiida is only poorly resolved very likely due to one or several rapid radiation events or due to the incomplete lineage sorting at the rRNA locus; and (5) the basal position of the genera *Chaenea* and *Trachelotractus* in molecular trees and phylogenetic networks is very likely a result of class III long-branch effects.

Key words: 18S rRNA gene; long-branch species; phylogenetic networks; quartet mapping; radiation; split spectrum.

Introduction

The Haptoria are free-living predatory ciliates living in terrestrial and aquatic habitats all around the world. Systematically, they belong to a highly diverse class Litostomatea which is morphologically well defined by having a special organelle, the dorsal brush, a telokinetal stomatogenesis, two transverse microtubule ribbons, and strongly developed postciliary microtubule ribbons, forming a plate-like structure in the cortex (Foissner 1996; Foissner and Foissner 1988; Leipe et al. 1992; Lipscomb and Riordan 1990; Lynn 2008). Molecularly, the Litostomatea are also well characterized by the deletion of the entire helix 23-5 in the 18S rRNA molecule (Strüder-Kypke et al. 2006; Vďačný et al. 2011a, b).

[1]Corresponding author; fax +421 2 60296333
e-mail vdacny@fns.uniba.sk (P. Vďačný).

http://dx.doi.org/10.1016/j.protis.2013.11.001

In contrast, the intraclass taxonomy of the Litostomatea poses great problems: the morphological and molecular data harmonize poorly and produce rather different classifications, depending on the authors and methods used (Foissner and Foissner 1988; Gao et al. 2008, 2010; Lipscomb and Riordan 1990, 1992; Lynn 2008; Strüder-Kypke et al. 2006; Vďačný et al. 2011a, b; Zhang et al. 2012). Based on these studies, Vďačný et al. (2011a, b) revised the litostomatean classification, using morphological and molecular methods. They concluded that (i) body polarization and simplification of the oral apparatus are main evolutionary trends in the Litostomatea and (ii) three distinct lineages (subclasses) occur: the Rhynchostomatia comprising the Tracheliida and Dileptida; the Haptoria comprising the Lacrymariida, Haptorida, Didiniida, Pleurostomatida, and Spathidiida; and the Trichostomatia uniting anaerobic endosymbionts in vertebrates. Further, they showed that (iii) the morphological "crown haptorids", viz., the complex dileptids, form the base of the litostomatean clade and (iv) the internal relationships of, especially, the Spathidiida remain obscure because many of them form separate branches within the basal polytomy of the order.

As the dileptids and pleurostomatids have shown, increased taxon sampling helps in defining molecular clades more clearly (Pan et al. 2010, 2013; Vďačný et al. 2011b). Thus, we analyzed the 18S rRNA gene of further "typical" haptorians, adding eight novel sequences to the available taxon sampling. Our rationale for selecting the newly sequenced species to improve the haptorian taxon sampling was based on the following assumptions. (i) *Spathidium foissneri* and *S. rectitoratum* are representative members of the name-bearing type genus *Spathidium* which defines the order Spathidiida according to the taxonomical principles. Thus, *Spathidium* sequences could contain some conserved plesiomorphies that would help to increase the statistical support for the monophyly of the order Spathidiida. (ii) *Arcuospathidium namibiense tristicha* and *Cultellothrix coemeterii* are morphologically more derived spathidiids. They could share some synapomorphies with other "crown" spathidiids already sequenced, and hence should help to improve resolution at least at some nodes within the order Spathidiida. (iii) *Lagynophrya acuminata* and *Acaryophrya* sp. are "traditional" haptorids, i.e., they exhibit some typical haptorid (e.g., meridionally arranged ciliary rows) as well as some typical spathidiid (e.g., three-rowed dorsal brush) features. Thus, these two sequences could help to increase resolution at the base of the Spathidiida and/or unravel relationships among the orders Spathidiida and Haptorida. (iv) As yet, only two "true" haptorid sequences have been available. Adding two further typical haptorids, *Fuscheria terricola* and *F. uluruensis*, could help to provide a stronger support for phylogenetic position of the order Haptorida within the subclass Haptoria.

Results

Phylogenetic Analyses

To determine the phylogenetic positions of the eight newly sequenced haptorians and to reconstruct the evolutionary history of the class Litostomatea, we analyzed four alignments using three phylogenetic methods (Bayesian inference, maximum likelihood and maximum parsimony) (Table 1). There are several monophyletic litostomatean lineages that were recognized in all alignments by all three statistical methods with very strong or full support (Figs 1–4): Rhynchostomatia, Trichostomatia, Haptorida, Lacrymariida, Pleurostomatida, and Didiniida. However, relationships between these monophyletic groups are very poorly resolved and vary according to the phylogenetic method used and the alignment analyzed (Figs 1–4, Supplementary Material Figs S1–S8). The basal position of the Rhynchostomatia is not shown in the trees rooted with out-group taxa (Figs 1 and 2), but cannot be excluded according to the statistical tree topology tests (Table 2). The Trichostomatia are nested within the Haptoria with full support in the Bayesian trees, and with poor to strong support (66–90%) in the ML trees, while they are depicted in the basal polytomy of the Litostomatea in the MP trees. Paraphyly or polyphyly of the Haptoria is shown in all trees, but monophyly of this subclass cannot be rejected by statistical tree topology tests (Table 2). Most obscure are phylogenetic relationships within the order Spathidiida which comprises spathidiids and several traditional haptorids, i.e., *Acaryophrya* sp., *Enchelyodon* sp. JF263446, *Enchelys* spp., *Lagynophrya acuminata*, and *Trachelophyllum* sp. No phylogenetic analysis was able to recover this order as monophyletic. In the MP trees, members of the order Spathidiida were consistently placed in the basal polytomy of the Haptoria, while in the Bayesian and ML trees they formed a paraphyletic assemblage together with trichostomatians. This grouping was strongly supported only in some Bayesian analyses (Figs 2–4), but it received a very poor support ranging from 30% to 35% bootstraps in the ML trees.

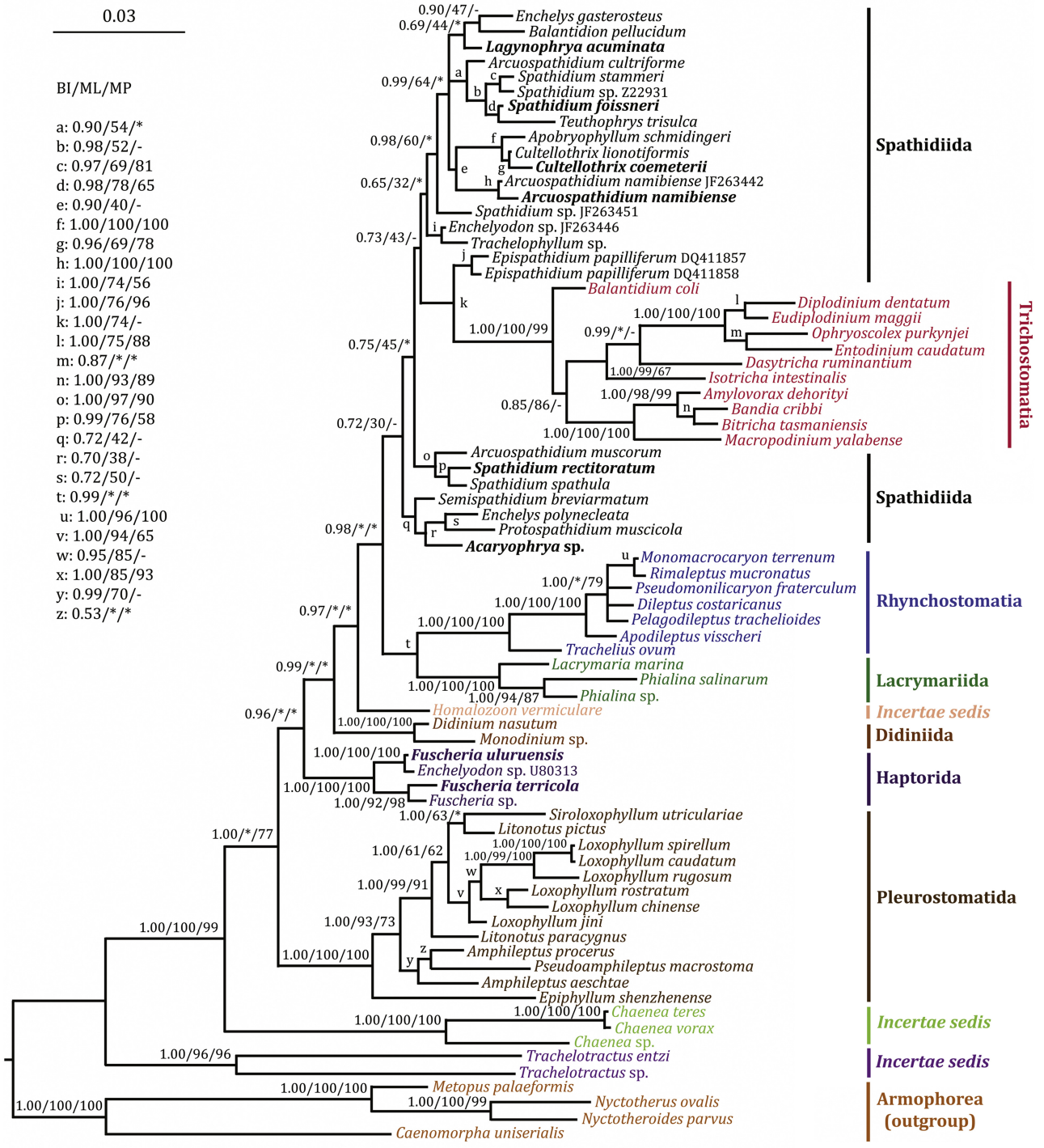

Figure 1. Small subunit rRNA gene phylogeny inferred from the ALL alignment (75 taxa and 1436 nucleotide characters). Results from the maximum likelihood (ML) and maximum parsimony (MP) bootstrap analyses were mapped onto the Bayesian inference (BI) tree. A dash indicates bootstrap values below 20%, while an asterisk indicates mismatch in branching pattern. Sequences in bold were obtained during this study. The scale bar indicates three substitutions per one hundred nucleotide positions.

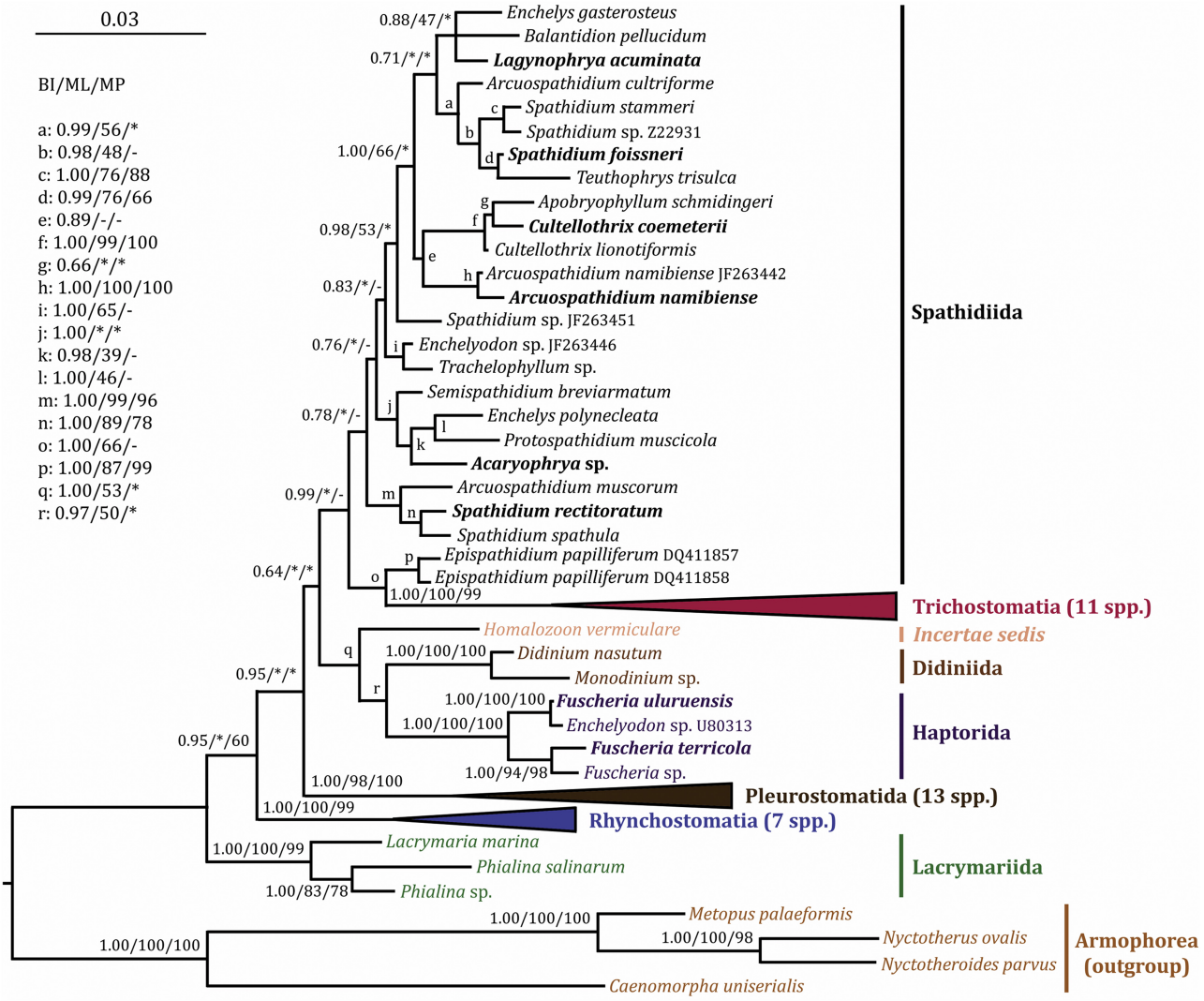

Figure 2. Small subunit rRNA gene phylogeny inferred from the WLBS alignment (70 taxa and 1459 nucleotide characters). Results from the maximum likelihood (ML) and maximum parsimony (MP) bootstrap analyses were mapped onto the Bayesian inference (BI) tree. A dash indicates bootstrap values below 20%, while an asterisk indicates mismatch in branching pattern. Sequences in bold were obtained during this study. The scale bar indicates three substitutions per one hundred nucleotide positions.

As concerns the phylogenetic placement of the eight newly sequenced haptorian taxa, the following results were obtained (Figs 1–4): (1) *Fuscheria terricola* and *F. uluruensis* cluster within the order Haptorida together with *Fuscheria* sp. and *Enchelyodon* sp. U80313 with full support from all statistical methods in all alignments analyzed; (2) *Spathidium rectitoratum* forms a strongly supported cluster together with *Spathidium spathula* and *Arcuospathidium muscorum* (invariably 1.00 PP, 97–100% ML, 90–99% MP); (3) *S. foissneri* is classified in a comparatively poorly supported clade together with *S. stammeri*, *Spathidium* sp. Z22931, and *Teuthophrys trisulca* (0.98–1.00 PP, 47–64% ML); (4) *Cultellothrix coemeterii* forms a monophylum with two other spathidiids having a laterally located dorsal brush, i.e., *C. lionotiformis* and *Apobryophyllum schmidingeri* (invariably 1.00 PP and 100% MP, 99–100% ML); and (5) phylogenetic positions of *Acaryophrya* sp., *Lagynophrya acuminata*, and the *Arcuospathidium namibiense* clones within the spathidiid cluster are usually very poorly resolved in all analyses.

Phylogenetic Networks

Traditional phylogenetic analyses assume that data have a tree-like structure of relationships and hence

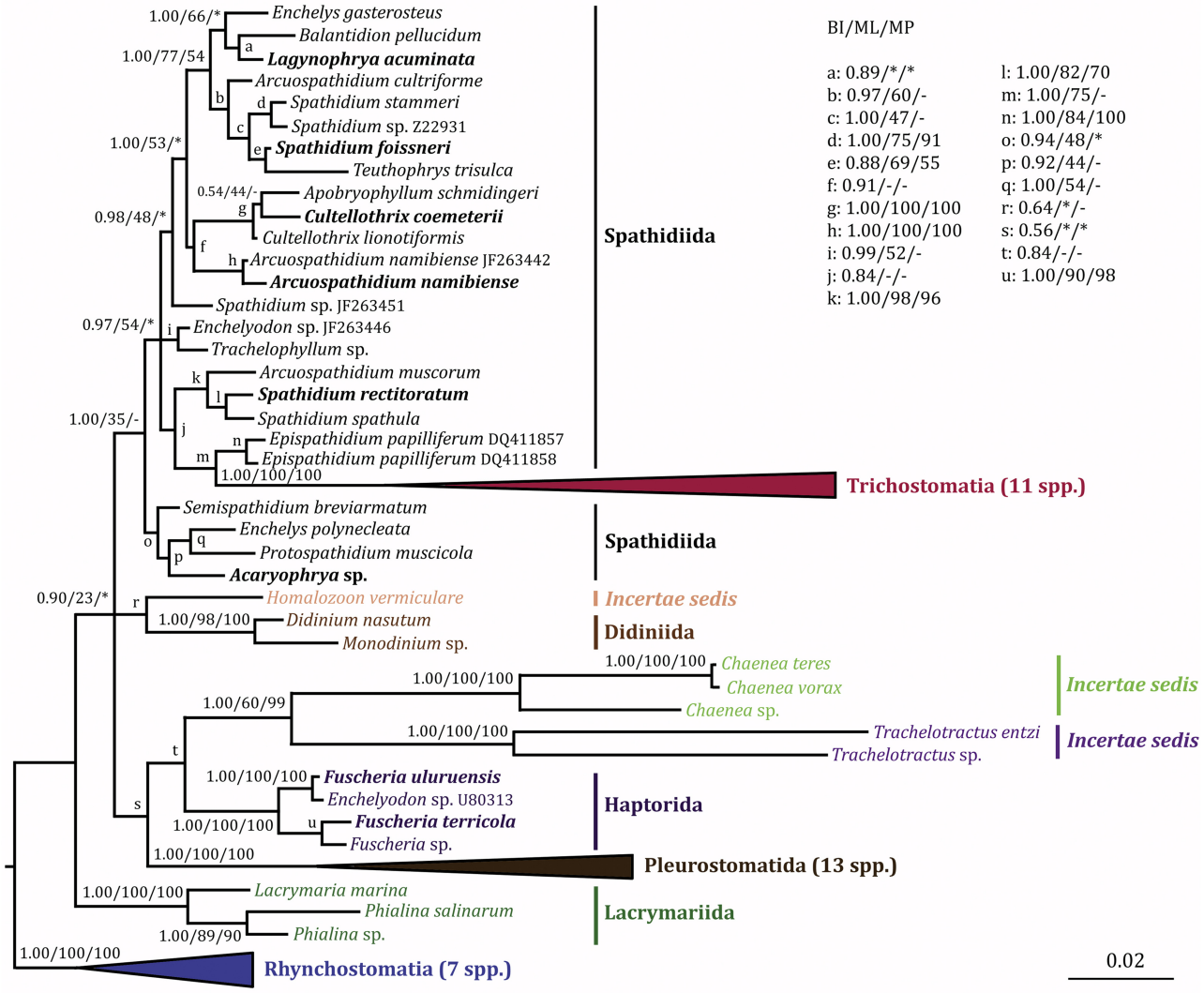

Figure 3. Small subunit rRNA gene phylogeny inferred from the LBS alignment (71 taxa and 1467 nucleotide characters). Results from the maximum likelihood (ML) and maximum parsimony (MP) bootstrap analyses were mapped onto the Bayesian inference (BI) tree. A dash indicates bootstrap values below 20%, while an asterisk indicates mismatch in branching pattern. Sequences in bold were obtained during this study. The scale bar indicates two substitutions per one hundred nucleotide positions.

force any data into a tree model, which is a fairly restrictive assumption. However, evolutionary histories of organisms are often much more complex than shown in binary trees (for an excellent review, see Morrison 2011). Phylogenetic networks are a powerful tool to visualize genealogical relationships among organisms without the restrictive supposition that the patterns must be tree-like (Huson et al. 2010). Specifically, phylogenetic networks diagram the conflicting as well as the consistent information and thus illustrate the alternative histories for different parts of the dataset (Hall 2011). In this way, we wanted to show all possible relationships within the litostomatean lineages and their statistical support.

The neighbornet graphs were calculated for all four alignments. The results were qualitatively very similar, therefore only phylogenetic networks inferred from the ALL and WO alignments are presented (Figs 5 and 6). Inclusion and exclusion of the out-group taxa and the long-branch in-group taxa (i.e., *Trachelotractus* and *Chaenea*) did not change the split graph patterns.

Network analyses show several monophyletic litostomatean lineages that are strongly supported with distinct sets of long parallel edges

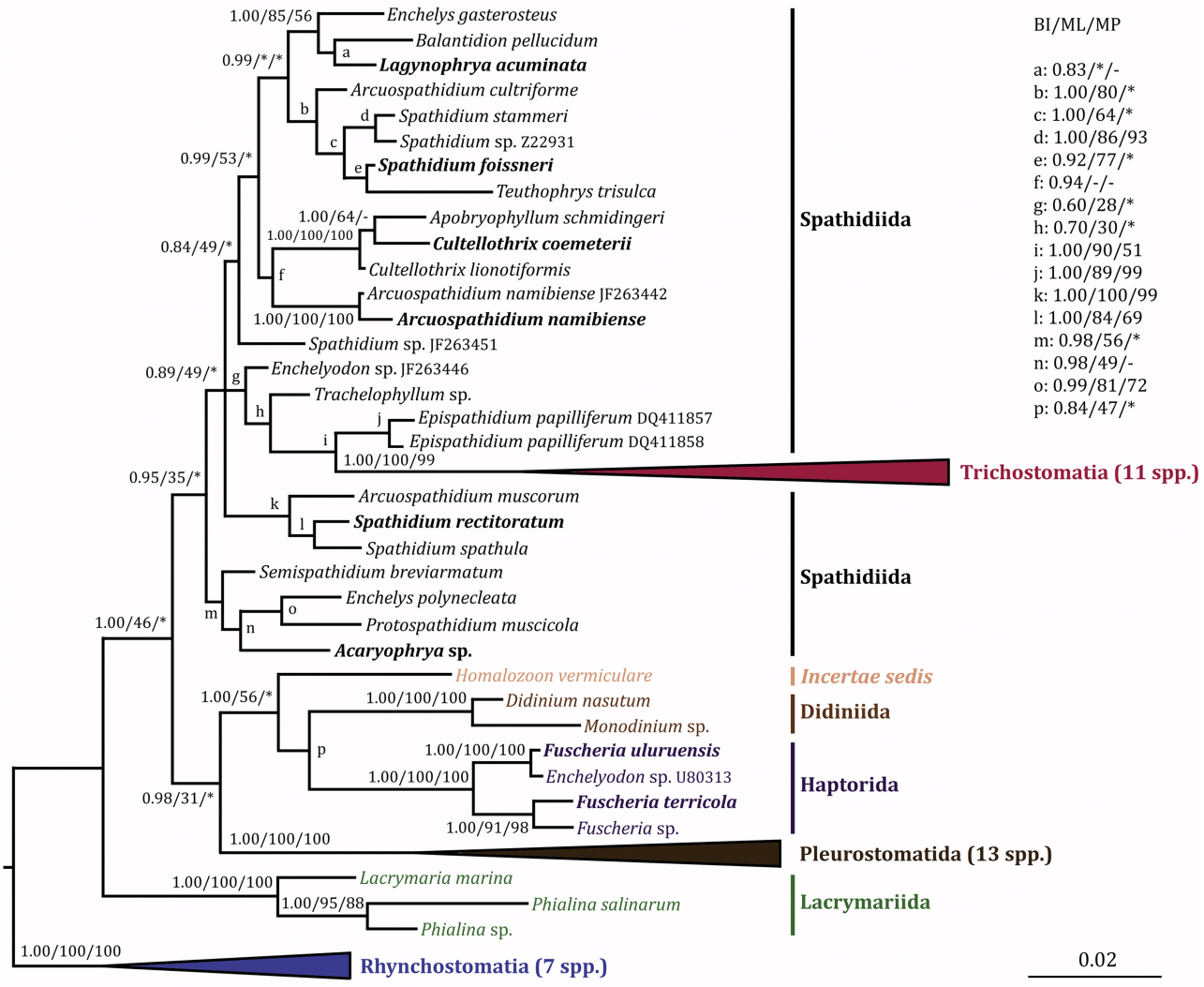

Figure 4. Small subunit rRNA gene phylogeny inferred from the WO alignment (66 taxa and 1510 nucleotide characters). Results from the maximum likelihood (ML) and maximum parsimony (MP) bootstrap analyses were mapped onto the Bayesian inference (BI) tree. A dash indicates bootstrap values below 20%, while an asterisk indicates mismatch in branching pattern. Sequences in bold were obtained during this study. The scale bar indicates two substitutions per one hundred nucleotide positions.

and bootstrap values ranging between 97% and 100%: Rhynchostomatia, Trichostomatia, Haptorida, Lacrymariida, Pleurostomatida, Didiniida, and the genera *Trachelotractus* and *Chaenea*. On the other hand, many short parallelograms in the star-like central part of the neighbornet graphs document considerable conflict in the phylogenetic signal for unambiguous resolution of the relationships between the litostomatean subclasses and haptorian orders. Furthermore, the signal for monophyly of the Spathiidida is not distinct, as this part of the network is not separated from the star-like central part by a set of long parallel edges, which indicates an explosive radiation or incomplete lineage sorting at the rRNA locus. Further, there is only a very weak support for classification of the Trichostomatia within the spathidiid cluster, as shown by several very short parallelograms connecting the trichostomatian clade with the two *Epispathidium papilliferum* isolates. On the other hand, there are also many short edges connecting the Trichostomatia with the Rhynchostomatia, a relationship not indicated in the binary phylogenetic trees.

As concerns the phylogenetic positions of the newly sequenced haptorian taxa, split graphs show similar results as phylogenetic trees. Specifically, *Fuscheria terricola* and *F. uluruensis* belong to the order Haptorida (100% BS), while the remaining

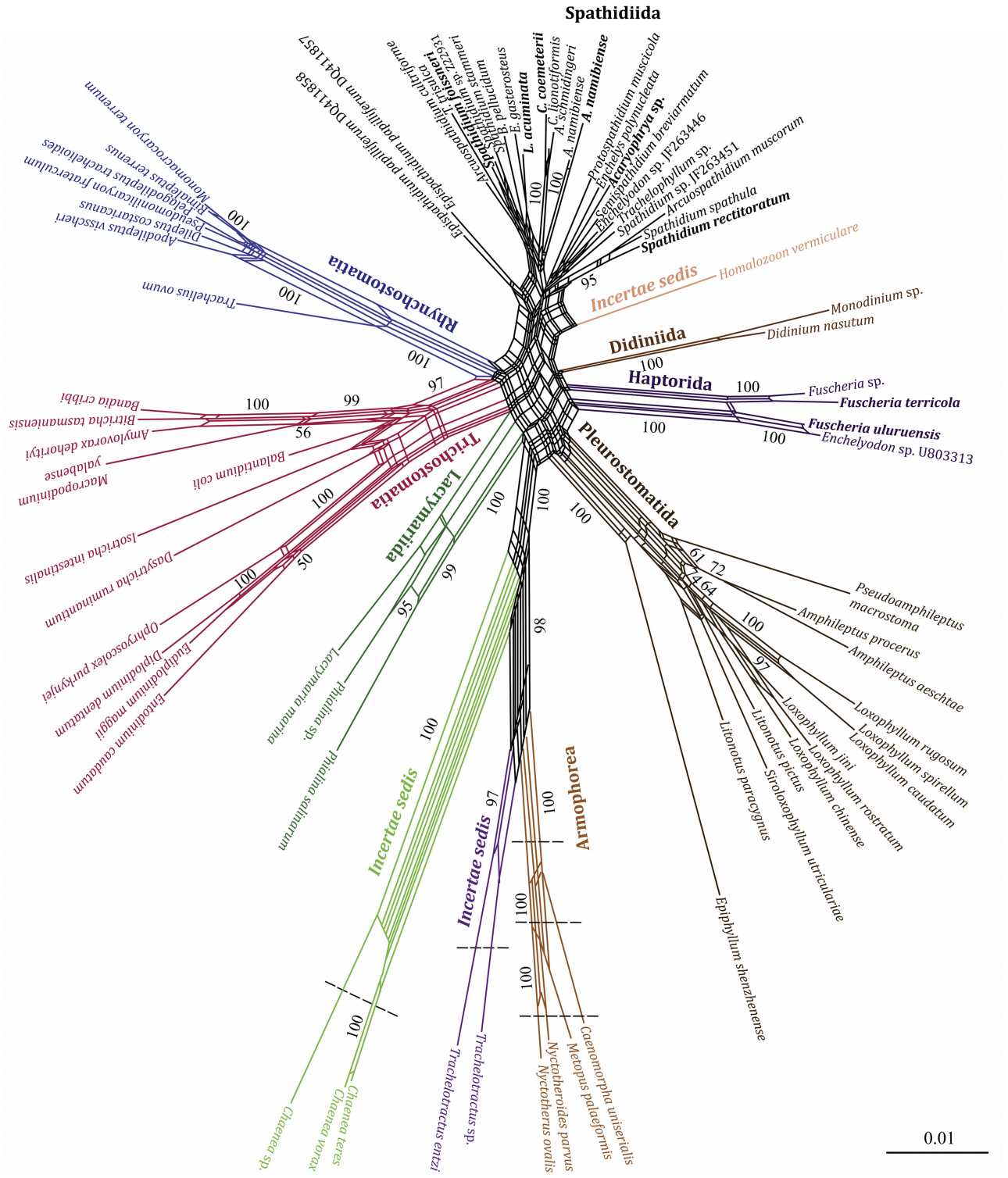

Figure 5. Phylogenetic network computed from the ALL alignment using the neighbornet algorithm and the uncorrected distances. Numbers along edges are bootstrap support values coming from 1000 replicates. Values $\leq$ 50% are not shown and some values > 50% in the spathidiid cluster are also omitted due to spatial constraints. Edges have been artificially shortened at dashed lines. Colour codes as in Figure 1. The scale bar indicates one substitution per one hundred nucleotide positions.

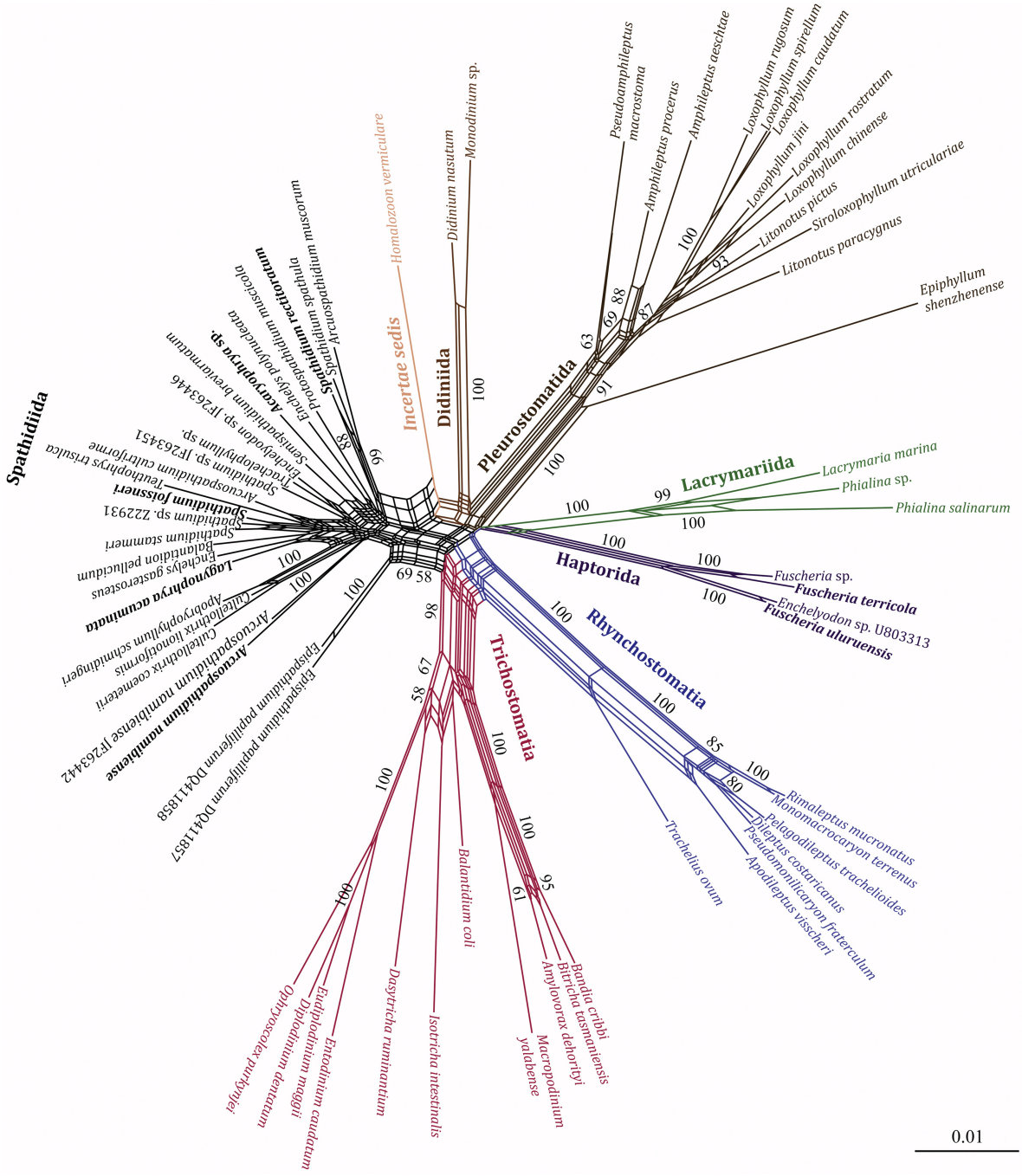

Figure 6. Phylogenetic network computed from the WO alignment using the neighbornet algorithm and the uncorrected distances. Numbers along edges are bootstrap support values coming from 1000 replicates. Values $\leq$ 50% are not shown and some values > 50% in the spathidiid cluster are also omitted due to spatial constraints. Colour codes as in Figure 4. The scale bar indicates one substitution per one hundred nucleotide positions.

species are placed within the spathidiid cluster (69% BS). *Spathidium rectitoratum* is depicted as most closely related to *Spathidium spathula* and *Arcuospathidium muscorum* (99% BS). *Spathidium foissneri* forms a poorly supported split together with *S. stammeri* and *Spathidium* sp. Z22931 (67% BS). On the other hand, *Cultellothrix coemeterii* forms a comparatively long and fully supported parallel split along with *C. lionotiformis* and *Apobryophyllum schmidingeri*. However, there is no

Table 1. Comparison of alignments and tree statistics for MP analyses.

Dataset	No. of taxa	No. of characters	In-group long branch species[a]	Out-group species[b]	No. of PIC[c]	No. of VC[c]	Length of tree	CI[d]	HI[d]	CIex[d]	RI[d]
ALL	75	1436	Included	Included	382	165	2227	0.3826	0.6174	0.3289	0.6502
WLBS	70	1459	Excluded	Included	360	127	1973	0.3832	0.6168	0.3371	0.6622
LBS	71	1467	Included	Excluded	342	164	2070	0.3657	0.6343	0.3057	0.6425
WO	66	1510	Excluded	Excluded	293	119	1815	0.3482	0.6518	0.2979	0.6665

[a]Species of the genera *Trachelotractus* and *Chaenea*.
[b]Armophorean taxa, i.e., *Caenomorpha uniserialis*, *Metopus palaeformis*, *Nyctotherus ovalis*, and *Nyctotheroides parvus*.
[c]PIC, parsimony informative characters; VC, variable characters.
[d]MP tree indices: CI, consistency index; CIex, consistency index excluding uninformative characters; HI, homplasy index; RI, retention index.

Table 2. Log likelihoods and *P*-values of AU (approximately unbiased), WSH (weighted Shimodaira-Hasegawa), and WKH (weighted Kishino-Hasegawa) tests for tree comparisons considering different topological scenarios. Significant differences (*P*-value < 0.05) between the best unconstrained and constrained topologies are in bold.

Topology	Alignment[b]	Log likelihood (–ln L)	Δ (–ln L)[c]	AU	WSH	WKH	Conclusion
Best maximum likelihood tree (unconstrained)	ALL	12,320.9384	–	0.937	0.985	0.883	–
	WLBS	11,252.0357	–	0.707	0.918	0.643	–
Rhynchostomatia sister to Haptoria + Trichostomatia	ALL	12,342.6178	21.68	0.144	0.245	0.085	Not rejected
	WLBS	11,257.2001	5.16	0.502	0.693	0.357	Not rejected
Monophyly of Haptoria[a]	ALL	12,349.8969	28.96	0.089	0.137	0.060	Not rejected
	WLBS	11,263.2827	11.25	0.232	0.417	0.222	Not rejected
Monophyly of *Trachelotractus* and *Chaenea*	ALL	12,341.9602	21.02	0.177	0.294	0.117	Not rejected

[a]As defined by Vďačný et al. (2011a) and including also *Trachelotractus* and *Chaenea*.
[b]ALL – alignment containing 75 taxa and 1436 characters (for details, see Fig. 1 and Table 1); WLBS – alignment containing 70 taxa and 1459 characters (for details, see Fig. 2 and Table 1).
[c]Difference between log likelihoods of constrained and best (unconstrained) tree.

split support for more reliable classification of *Acaryophrya* sp., *Lagynophrya acuminata*, and the *Arcuospathidium namibiense* clones within the spathidiid cluster (Fig. 6).

Split Spectra

Conventional tree-construction methods cannot detect the signal to noise ratio in the data. Split spectrum analysis is an ideal tool for estimation of information content in the alignment. This approach is independent of evolutionary substitution models and tree-building algorithms, and thus directly visualizes how much untransformed signal-like information is present in the dataset (Wägele and Rödding 1998). In this way, split spectrum analysis helps to reveal which high bootstrap or posterior probability values can result from chance similarities (Wägele et al. 2009). Further, this method is useful to discover long branch artefacts, as shown by Wägele and Mayer (2007). Based on the split support spectrum, they discerned three classes of long branch effects.

To reveal the signal to noise ratio and to detect the long branch effects, we have computed split spectra (i.e., numbers of clade-supporting positions) for the ALL and WO alignments. Figure 7 shows the first 20 splits with the highest support for each alignment. In the ALL alignment, four very strongly supported splits are identified (Fig. 7A). The best split contains Armophorea (8 binary, 25 asymmetric and 27 noisy positions) on one hand and Litostomatea (8 binary, 5 asymmetric and 41 noisy positions) on the other one. The next column represents the split between *Caenomorpha* and Litostomatea (13 binary and 41 asymmetric positions) vs. *Metopus*, *Nyctotherus* and *Nyctotheroides* (13 binary, 1 asymmetric and 45 noisy positions). Split no. 3 supports monophyly of the genus *Chaenea* with 14 binary and 32 asymmetric positions. Split no. 4 is the last very strongly supported bipartition in Litostomatea {excl. *Trachelotractus* spp.} (4 binary, 3 asymmetric and 35 noisy positions) vs. Armophorea + *Trachelotractus* spp. (4 binary, 9 asymmetric and 15 noisy positions). However, the majority of the following splits are mutually incompatible (e.g., splits nos 5, 6, 8, 9, 11, 13–18, 20), which is a result of random attraction of in-group (*Chaenea* spp. and *Trachelotractus* spp.) or out-group (*Caenomorpha uniserialis*) long-branch species to other taxa. Such a split spectrum, with a large number of mutually incompatible and strongly supported groupings, is clear evidence for class III long-branch effects according to Wägele and Mayer (2007).

Split spectra clearly improve after removal of all long branch species (Fig. 7B), since there are much less mutually incompatible splits and strongly supported splits that are in conflict with phylogenetic tree shown in Figure 4. However, there are still some nonsense splits but these are much less strongly supported than those in Figure 7A. Furthermore, support for the nonsense splits in Figure 7B comes mostly from noise positions (vs. asymmetric positions in Fig. 7A) and these splits are caused by random attraction of various taxa (vs. by attraction of mostly three taxa, *Caenomorpha*, *Chaenea* and *Trachelotractus* spp., in Fig. 7A). This indicates that the nonsense splits in Figure 7B are results of chance similarities rather than long-branch effects. By contrast to the split spectrum in Figure 7A, there are conserved nucleotide patterns detected for several deeper nodes, especially at ordinal rank, in the split spectrum presented in Figure 7B. The best split contains a clade uniting didiniids (1 binary and 36 asymmetric positions) vs. all other litostomatean taxa (1 binary and 12 noisy positions). The second best split represents the bipartition in rhynchostomatians vs. all other litostomateans, with 2 binary and 25 noisy positions supporting the functional in-group and 2 binary, 17 asymmetric and 7 noisy positions supporting the functional out-group. Distinct nucleotide patterns supporting all free-living litostomatean orders, except for the Spathidiida, can be found within the first 20 splits with total support ranging from 25 (Lacrymariida vs. the rest) to 32 (Haptorida vs. the rest). Separation of *Epispathidium papilliferum* isolates and the Trichostomatia from all other litostomateans has a total support of only 4, with 1 asymmetric and 3 noisy positions supporting the functional in-group and 1 noisy position supporting the functional out-group. No split with conserved primary homologies supporting the Spathidiida clade is present within 200 best splits.

To summarize, the present split spectrum analysis documents that the high posterior probability and bootstrap values for monophylies of the Rhynchostomatia, Trichostomatia, Haptorida, Lacrymariida, Pleurostomatida, and Didiniida are based on conserved nucleotide primary homologies. On the other hand, the high posterior probabilities for classification of the Trichostomatia within the Spathidiida are very likely a result of chance similarities. Another explanation for the poor support of the Trichostomatia-Spathidiida grouping in the split spectrum analysis is an explosive radiation within the Spathidiida or incomplete lineage sorting at the rRNA locus. This caused that only a very few conserved apomorphies are shared

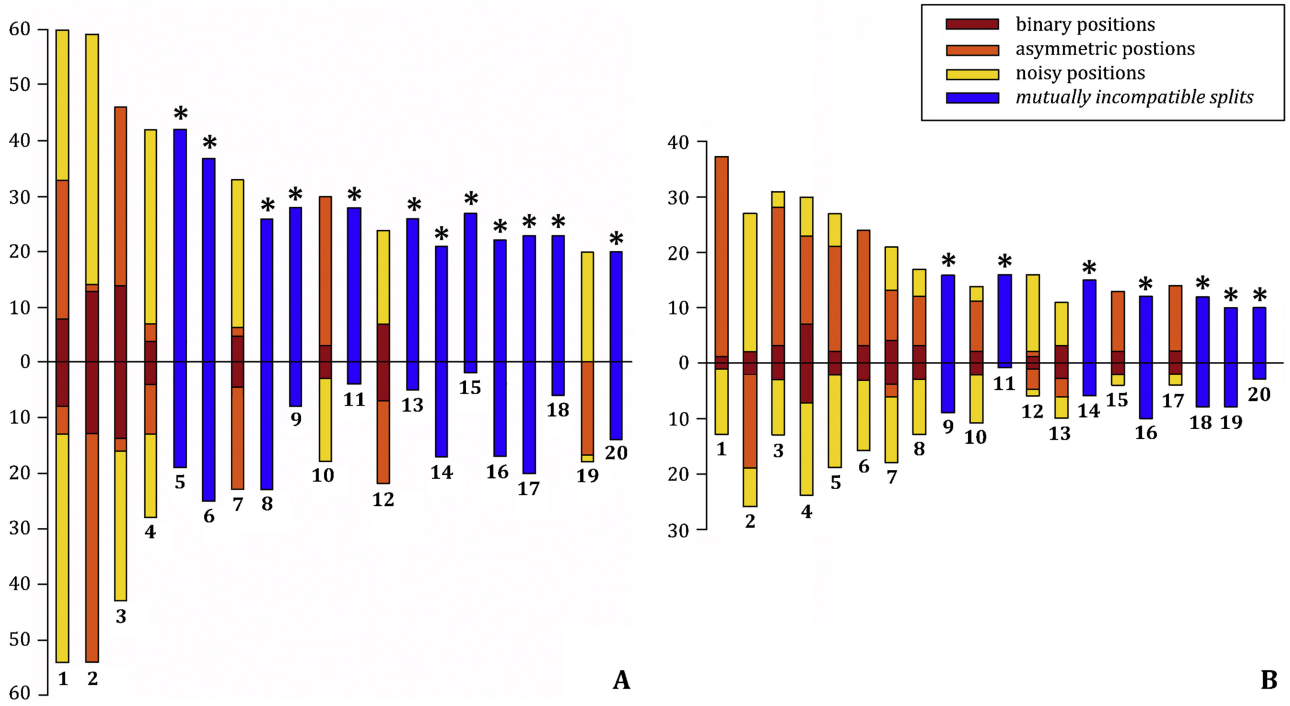

Figure 7. Split support spectrum for the ALL (**A**) and WO (**B**) alignments. Column height represents the number of clade-supporting positions, i.e., putative primary homologies. Column parts above the y-axis represent the in-group partition, while those below the axis correspond to the out-group partition. Columns marked by an asterisk represent splits that are mutually incompatible. The first spectrum (**A**) contains the following partitions (only functional in-groups are listed): **1:** Armophorea; **2:** *Caenomorpha* + Litostomatea; **3:** *Chaenea* spp.; **4:** Litostomatea {excl. *Trachelotractus* spp.}; **5:** Armophorea + Litostomatea {excl. *Chaenea* and *Trachelotractus* spp.}; **6:** Litostomatea {excl. *Trachelotractus* sp.}; **7:** Armophorea + Litostomatea {excl. *Trachelotractus* spp.}; **8:** *Caenomorpha* + Litostomatea {excl. *Trachelotractus* sp.}; **9:** Armophorea {excl. *Caenomorpha*} + Litostomatea {excl. *Trachelotractus* sp.}; **10:** *Chaenea teres* + *C. vorax*; **11:** Armophorea {excl. *Caenomorpha* and *Metopus*} + Litostomatea; **12:** Armophorea {excl. *Nyctotherus* and *Nyctotheroides*} + Litostomatea; **13:** Armophorea {excl. *Caenomorpha* and *Nyctotheroides*} + Litostomatea; **14:** *Caenomorpha* + Litostomatea {excl. *Trachelotractus* spp.}; **15:** *Metopus* + *Nyctotheroides* + Litostomatea; **16:** Litostomatea {excl. *Trachelotractus entzi*}; **17:** *Chaenea* spp. + *Trachelotractus entzi*; **18:** *Metopus* + *Nyctotheroides* + Litostomatea {excl. *Trachelotractus* spp.}; **19:** Armophorea + Litostomatea {excl. Haptorida}; **20:** *Chaenea* spp. + *Caenomorpha*. The second spectrum (**B**) contains the following partitions (only functional in-groups are listed): **1:** Didiniida; **2:** Rhynchostomatia; **3:** Haptorida; **4:** Pleurostomatida; **5:** Dileptida; **6:** Lacrymariida; **7:** *Amylovorax* + *Bandia* + *Bitricha* + *Macropodinium*; **8:** *Psedoamphileptus* + *Amphileptus* spp. + Litonotidae; **9:** *Monodinium* + Lacrymariida; **10:** *Diplodinium* + *Eudiplodinium* + *Ophryoscolex* + *Entodinium*; **11:** Haptorida + *Dasytricha*; **12:** Rhynchostomatia + Lacrymariida + Haptorida + Didiniida + *Homalozoon* + Spathidiida; **13:** Rhynchostomatia + Lacrymariida + Haptorida + Didiniida + *Homalozoon* + Spathidiida + *Balantidium*; **14:** Haptorida + *Phialina salinarum*; **15:** *Arcuospathidium namibiense* clones; **16:** Rhynchostomatia + *Lacrymaria marina*; **17:** *Phialina salinarum* + *Phialina* sp.; **18:** Rhynchostomatia + *Phialina* sp.; **19:** Rhynchostomatia + *Didinium*; **20:** Haptorida + *Litonotus paracygnus*.

among spathidiids and between spathidiids and trichostomatians.

Four-Cluster Likelihood Analyses

To explore the potential of conflicting signal in the 18S rRNA gene to resolve phylogenetic relationships among litostomatean lineages, we have performed the four-cluster likelihood analysis. When considering four taxa groups, there are three possible tree topologies. The relative frequencies of the likelihoods for each topology are plotted in an equilateral triangle. The three tips of the triangle represent the percentage of the three well-resolved quartets. Three rectangles on the sides of the triangle are quartets with network evolution,

i.e., with conflicting signal. The central region of the triangle represents star-like evolution, i.e., noisy signal (Nieselt-Struwe and von Haeseler 2001). This method has the advantage that it directly tests support for an interior branch without any reference to phylogenetic structure within predefined groups. This effectively leads to a reduction of noise (Wägele et al. 2009).

As concerns the ALL and WLBS alignments, we divided the species into four clades: (a) Rhynchostomatia [designated as R] including tracheliid and dileptid sequences; (b) Haptoria [designated as H] including pleurostomatid, didiniid, lacrymariid, haptorid, and spathidiid sequences; (c) Trichostomatia [designated as T] including sequences from endosymbiotic anaerobic litostomateans; and (d) out-group [designated as O] including the four armophorean sequences. In the WO alignment, we recognized the following four clades: (a) Rhynchostomatia [designated as R]; (b) Trichostomatia [designated as T]; (c) Spathidiida [designated as S]; and (d) Haptorida sensu lato [designated as H s.l.] including pleurostomatid, didiniid, lacrymariid, and haptorid sequences. Between the four suggested clades three possible and competing relationships were generated, each represented by a tip of the triangle. The quartet puzzling analysis of all three alignments shows that there are almost no unresolved quartets in the central triangle (0.2% for the WO alignmnent and 0.4% for the ALL and WLBS alignment each). Signal for partly resolved quartets is between 0.6% and 2.7% in the three rectangles on the sides of the triangle, being well bellow the "high" threshold of 20–30% (Lemey et al. 2009). This shows that all three alignments are suitable to resolve phylogenetic relationships between the three litostomatean subclasses.

In the ALL alignment, the basal position of the Rhynchostomatia and sister relationship of the Haptoria and Trichostomatia is the most favoured topology supported by 56.5% of data points falling on or near the left tip of the triangle (Fig. 8A). When the long-branch haptorian taxa (i.e., *Trachelotractus* and *Chaenea* spp.) are excluded from the dataset, support for this topology increases to 67.6% (Fig. 8B).

When the out-group taxa were excluded, the monophyly of the Haptoria, i.e., sister relationship of the spathidiids and haptorids *s.l.*, could be explored. The quartet mapping analyses supports the monophyly of the Haptoria by 49% of data points. On the other hand, the paraphyly of the Haptoria is represented by a signal for either a sister relationship between spathidiids and trichostomatians (29.7% of data points) or a sister relationship between haptorids *s.l.* and trichostomatians (21.3% of data points). If these two possibilities are added up, then the paraphyly of the Haptoria is supported by 51% of data points (Fig. 8C).

To summarize, according to the present quartet mapping analyses, it is not possible to unambiguously decide whether there is a distinct signal in the 18S rRNA gene for monophyly (49%) or paraphyly (51%) of the Haptoria (Fig. 8C). If the monophyly, of the Haptoria is anticipated, which is not rejected by the statistical tree topology tests (Table 2), then the Rhynchostomatia would be the basal litostomatean subclass and the Haptoria and Trichostomatia would be sister groups according to the present four-cluster likelihood analyses (Fig. 8A and 8B).

Discussion

Chaos in the Phylogeny of the Order Spathidiida

The order Spathidiida unites holotrichously ciliated haptorians with bursiform to spatulate body, typically three-rowed dorsal brush, and usually anteriorly curved ciliary rows (Foissner and Xu 2007). Recent molecular studies have indicated that also trachelophyllids and several "traditional" haptorids belong to this taxonomically difficult assemblage (Vďačný et al. 2011a, 2012). Phylogenetic relationships among spathidiids are the worst resolved part of the litostomatean tree of life, having short internodes and many poorly statistically supported deeper nodes (Figs 1–4). In the neighbornet graphs, spathidiid taxa are typically connected with many short parallelograms, causing this part of the phylogenetic networks to almost completely lack treeness (Figs 5 and 6). Likewise, few or no conserved primary homologies supporting deeper nodes within the spathidiid clade are found in the present split spectrum analysis (Fig. 7). This indicates that 18S rRNA gene per se is very likely insufficient to resolve the deep spathidiid phylogeny. Possibly, further loci can help to improve resolution within the spathidiid lineages. But another four molecular markers (ITS1, 5.8S rRNA, ITS2, and first two domains of the 28S rRNA gene) did not bring distinctly better-supported spathidiid phylogenies (Vďačný et al. 2012). This can be explained by one or several rapid radiation events that did not allow primary nucleotide homologies for deeper branching spathidiid nodes to be fixed. However, the signature of explosive radiation would be an insufficient number of phylogenetically

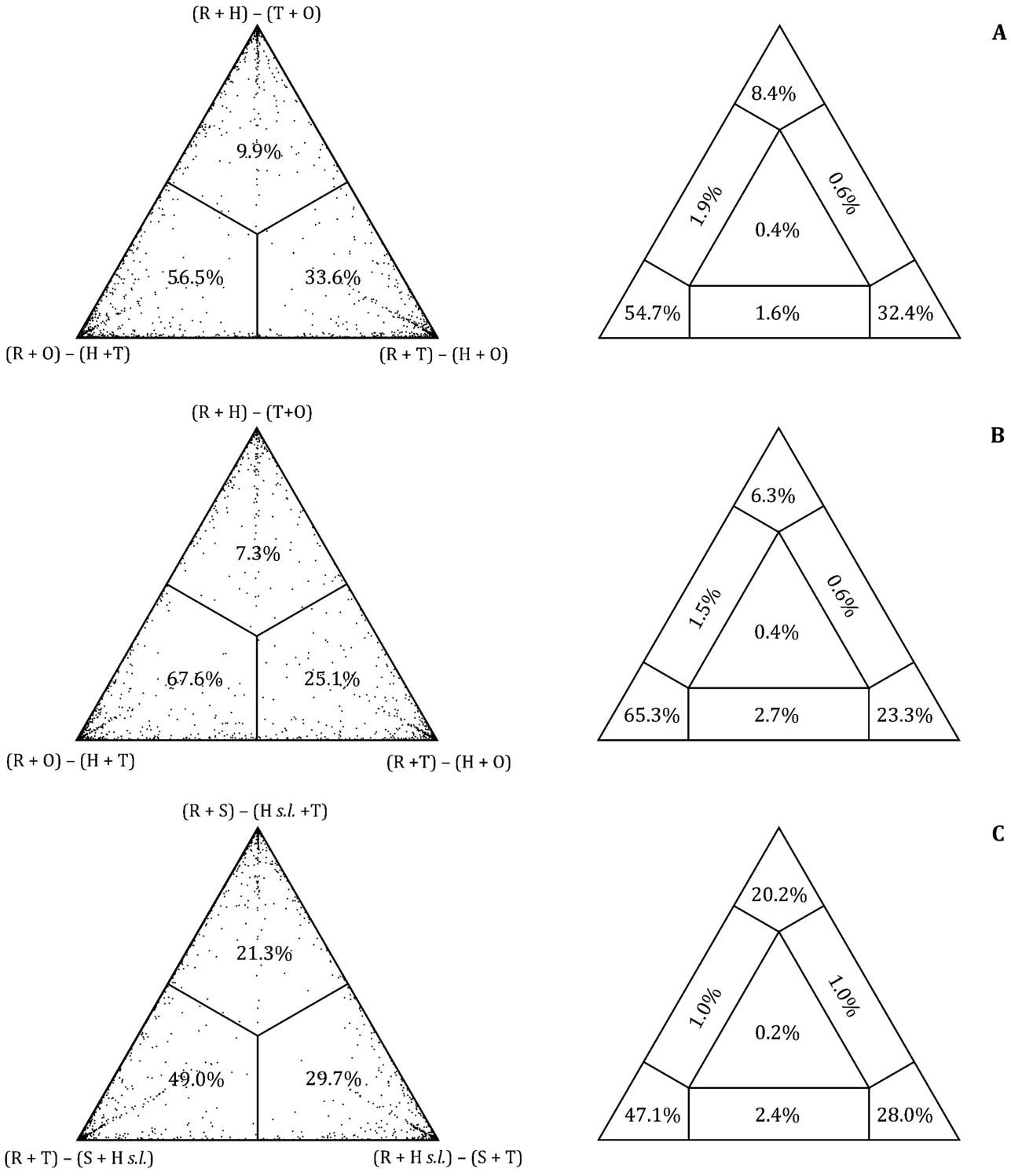

Figure 8. Quartet likelihood mapping showing distribution of phylogenetic signal for three possible relationships among litostomatean subclasses. The corners of the triangles show the percentage of fully resolved trees. The rectangular areas show the percentage of trees that are in conflict. The central triangle shows the percentage of unresolved star-like trees. The studied alignments are: ALL (A), WLBS (B), and WO (C). H – Haptoria, H s.l. – Haptorida sensu lato, O – out-group, R – Rhynchostomatia, S – Spathidiida, T – Trichostomatia.

informative characters, which in turn would produce truly unresolved quartets in quartet puzzling analyses. As this is not the case, another explanation for the poorly supported spathidiid phylogeny is the incomplete lineage sorting at the rRNA locus. A promising solution to unravel the evolutionary history of the spathidiids could be the synergistic effect of combining molecular and morphological datasets into a single supermatrix. This approach has, indeed, shown that some deep branching spathidiid nodes can be more reliably resolved and statistically supported (Vďačný and Foissner 2013).

Long-branch Effects of *Chaenea* and *Trachelotractus*

The genera *Chaenea* and *Trachelotractus* display a simple bursiform morphology, appearing, at first glance, as typical haptorids. However, both genera are placed as long branches at the base of the Litostomatea far away from members of the order Haptorida both in the phylogenetic trees (Fig. 1) and the neighbornet graphs (Fig. 5). Spectral analyses show that *Chaenea* and *Trachelotractus* species form a large number of mutually incompatible but strongly supported splits with various armophorean and litostomatean taxa (Fig. 7A). Such a split spectrum is clear evidence for class III long-branch effects. According to Wägele and Mayer (2007), the basic cause for class III effects is that homoplasies outnumber apomorphies. This leads to nonsense clades that are supported only by chance and attracted due to non-homologous similarities. Thus, the basal position of *Chaenea* and *Trachelotractus* in the phylogenetic trees is very likely due to the attraction by long branches of the out-group taxa. This is also indicated by the statistical tree topology tests that do not reject the sister relationship of *Chaenea* and *Trachelotractus* as well as their classification within the monophyletic Haptoria (Table 2). Therefore, based on the morphology and present phylogenetic analyses, we believe that the basal position of these two genera is very likely artificial and their inclusion into analyses may distort the true phylogeny (Kück et al. 2012; Wägele and Mayer 2007).

Affiliation of *Chaenea* and *Trachelotractus* within the Haptoria can be, at the present state of knowledge, deduced only from specialities of their ciliary pattern. *Chaenea* shares some conspicuous morphological peculiarities with lacrymariids, as already recognized by Vďačný et al. (2011a). Specifically, *Chaenea* and lacrymariids exhibit a dorsal brush that is distinctly separated from the anterior body end by files of narrowly spaced somatic monokinetids. These are slightly helically arranged in *Chaenea*, while distinctly helical forming head kineties in lacrymariids (Foissner 1984). On the other hand, the dorsal brush of *Trachelotractus* is two-rowed (Foissner 1997; Long et al. 2009), a unique feature typical for the family Fuscheriidae of the order Haptorida (Foissner and Foissner 1988; Foissner et al. 2002; Gabilondo and Foissner 2009). This indicates that *Trachelotractus* could be a fast-evolving member of the Haptorida.

Basal Position of the Subclass Rhynchostomatia

Rhynchostomatians are free-living predators characterized by a ventrally located oral opening at the base of a proboscis that carries a complex oral ciliature, including circumoral kinety (∼ paroral membrane) and many preoral kineties (∼ adoral organelles) (for a review, see Vďačný and Foissner 2012). According to the comparative morphological analyses, rhynchostomatians are morphologically nearest to the last common progenitor of the Litostomatea because their oral apparatus exhibits several important plesiomorphic features, viz., the ventrally located oral opening and the presence of many preoral kineties (Vďačný et al. 2010, 2011a, b, 2012). However, basal position of the rhynchostomatians is not recognized in molecular trees when long-branch taxa are included into the analyses (e.g., Pan et al. 2013; Zhang et al. 2012; Fig. 1). A similar scenario is observed in some trees also when long-branch species are excluded from the phylogenetic inferences (Fig. 2). But than the nodal support for all deep branching nodes is very poor, indicating a basal polytomy in the Litostomatea. On the other hand, the present quartet-mapping likelihood analyses support most the topology in which rhynchostomatians represent the basal litostomatean group. Specifically, their pivotal position is supported with 56.5% of data points when long-branch species are included (Fig. 8A), but with 67.5% when long-branch species are excluded (Fig. 8B). Further, according to the statistical topology tests, the basal position of the rhynchostomatians within the Litostomatea cannot be excluded in trees inferred from alignments containing and also lacking long-branch in-group species (Table 2). Thus, based on the body of evidence from morphology, quartet likelihood mapping, and statistical topology tests, we find the rhynchostomatians as the best candidates for the basal litostomateans.

Phylogenetic Position of the Subclass Trichostomatia

The subclass Trichostomatia comprises anaerobic endocommensals or parasites in vertebrates, ranging from fish to reptiles and mammals (Lynn 2008). Trichostomatians have never been depicted as a sister group of the free-living litostomateans in phylogenetic trees, but have been usually nested deep within one of the haptorian orders, the rapacious Spathidiida. Specifically, they have been placed as a sister taxon of the *Epispathidium papilliferum* isolates (e.g., Gao et al. 2008; Pan et al. 2010; Strüder-Kypke et al. 2006, 2007; Vďačný et al. 2010, 2011a, b, 2012). However, this grouping is supported only with four nucleotide positions of which three are even noisy according to the present analysis of split spectra. Further, the present statistical topology tests do not reject trees in which the Trichostomatia cluster as a sister group of the Haptoria (Table 2). We have obtained very similar results also from the four-cluster likelihood analyses in which the sister relationship of the Trichostomatia and Haptoria is supported with 49% of data points, while the sister relationship of the Trichostomatia and Spathidiida is supported by only 29.7% of data points, and the sister relationship of the Trichostomatia and Haptorida sensu lato by only 21.3% (Fig. 8C). However, in molecular phylogenies, the Trichostomatia form comparatively long branches, which indicates that they are fast-evolving and thus that very few conserved plesiomorphies will be shared with the rest of the Spathidiida. This, in turn, can explain why the clustering of the Trichostomatia within the Spathidiida is so weakly supported in the split spectrum analyses, and why the sister relationship of the Trichostomatia and Haptoria is not excluded by the tree topology tests. To sum up, there is no distinct signal in the 18S rRNA gene to solve unambiguously the phylogenetic position of the Trichostomatia. Thus, the traditional morphology-based classifications of the trichostomatians and the haptorians as a distinct subclass each cannot be rejected at the present state of knowledge (e.g., Foissner and Foissner 1988; Grain 1994; Jankowski 2007; Lynn 2008).

Methods

Collection, sample processing and sequencing: Eight haptorian species were collected from a variety of habitats and countries (Table 3). Depending on collection circumstances and abundance of the species, specimens were either picked directly from the environmental samples or were cultivated, and then were used for the molecular investigations. For description of culture methods, see Vďačný and Foissner (2012). The species mentioned in this study were identified by combining live observation with protargol impregnation and scanning electron microscopy, as described in Vďačný and Foissner (2012). From each studied species, about 16–80 specimens were picked with a micropipette and stored in ATL buffer (Table 3). Their genomic DNA was extracted with DNEasy Tissue Kit (Qiagen, Hildesheim, Germany). PCR and sequencing conditions followed Foissner et al. (2011).

Sequence alignments: To unravel the evolutionary history of litostomateans and to study the effect of taxon sampling on it, we prepared four different datasets that were used for construction of 18S rRNA gene alignments (Table 1). The first dataset was designated as ALL and comprised four out-group armophorean taxa and 71 in-group litostomatean taxa, including five long branch species from the genera *Trachelotractus* and *Chaenea*. All sequences, except for those obtained in this study, were retrieved from GenBank (Supplementary Table 1). In the second dataset WLBS, we excluded the five problematic in-group species to study their influence on resolution of the litostomatean phylogenetic interrelationships. Since the out-group taxa were also shown as long branches in respect to the litostomatean sequences, we prepared a third dataset, designated as LBS, without the four armophorean out-group sequences but with the long branch in-group sequences. The last fourth dataset WO served to reveal the effect of all long branch taxa on reconstruction of the litostomatean phylogenetic relationships. To this end, both the four out-group taxa and the five long branch in-group taxa were excluded.

Alignments from all four datasets were created in MAFFT ver. 6.5 using the Q-INS-i strategy that considers the secondary structure of the 18S rRNA molecule (Katoh and Toh 2008). The resulting alignments were checked, refined, and masked manually, following the column scores calculated by the computer program G-blocks ver. 0.91b (Castresana 2000; Talavera and Castresana 2007).

Phylogenetic analyses: To determine the phylogenetic positions of the eight newly sequenced haptorian species within the class Litostomatea, we analyzed four datasets containing 18S rRNA gene sequences from all major litostomatean lineages (Tables 1 and 3). For all alignments the GTR + I + Γ evolutionary model was the best fitted model selected by jModeltest ver. 0.1.1 under both the Akaike and the Bayesian Information Criterion (Guindon and Gascuel 2003; Posada 2008). This model was implemented in MrBayes ver. 3.2.1 (Ronquist and Huelsenbeck 2003) on the CIPRES Portal ver. 1.15 (Miller et al. 2009). Two parallel runs with four MCMC chains (one cold and three heated) began with random starting trees. They were run for five million generations with trees saved every 100 generations until the average deviation of split frequencies fell well below 0.01. The first 12,500 trees sampled before stationary were discarded as burn-in. Posterior probabilities of the phylogenies and their branch lengths were estimated from the remaining trees. The maximum likelihood (ML) analyses were also conducted online on the CIPRES Portal using the RAxML algorithm with the default GTRGAMMA + I model (Stamatakis et al. 2008). Maximum parsimony (MP) trees were constructed in PAUP* ver. 4.0b8 using a heuristic search with the NNI swapping algorithm and 10 random sequence addition replicates (Swofford 2003). The reliability of the internal branches in the ML and MP trees was assessed by the non-parametric bootstrap approach with 1000 replicates. Results from the ML and MP bootstrap analyses were mapped onto the Bayesian inference trees.

Tree topology tests: Opposite to the topology of the best-scoring unconstrained ML trees inferred from the ALL and

Table 3. Characterization of new 18S rRNA gene sequences of 8 litostomatean ciliates (arranged alphabetically).

Taxon	Collection site	No. of cells picked	Sequence length (nt)	GC content (%)	GenBank entry
Acaryophrya sp.	Soil from Chobe River floodplain, Botswana	16	1595	42.82	KF733758
Arcuospathidium namibiense tristicha Foissner et al., 2002[a,b]	Moss, Germany	20	1594	42.72	KF733754
Cultellothrix coemeterii (Kahl, 1943) Foissner and Xu, 2007[b]	Coniferous litter from the surroundings of Oslo, Norway	30	1594	42.97	KF733755
Fuscheria terricola Berger et al., 1983	Bromeliad litter from Botanical Garden, Rio de Janeiro, Brazil	70	1593	42.12	JQ723965
Fuscheria uluruensis Foissner and Gabilondo, 2009 in Gabilondo and Foissner, 2009	Mud and soil from an ephemeral pool on the Ayers Rock, Australia	22	1592	42.02	KF733753
Lagynophrya acuminata Kahl, 1935	Mud from bamboo stump, Jamaica	80	1595	43.26	JQ723972
Spathidium foissneri Hlúbiková et al., 2006 in Vďačný et al., 2006[c]	Soil of an ephemerally flooded lawn, Idaho, USA	70	1595	43.13	KF733756
Spathidium rectitoratum Kahl, 1930	Coniferous litter from the surroundings of Oslo, Norway	30	1597	42.70	KF733757

[a]Specimens from the same population were first investigated by Vďačný et al. (2011a).
[b]Sample collected by Mr. Hippe.
[c]Sample collected by Dr. Bourland.

WLBS alignments, three constraints were forced on both alignments: (1) basal position of the subclass Rhynchostomatia, i.e., a sister relationship of the Rhynchostomatia and the Haptoria + Trichostomatia; (2) monophyly of the subclass Haptoria; and (3) monophyly of *Trachelotractus* and *Chaenea* (Table 2). Trees were constructed using the ML criterion and a heuristic search with the NNI swapping algorithm and 10 random sequence addition replicates. Per-site log likelihoods were computed for all trees in PAUP* under the substitution evolutionary models calculated by jModeltest. CONSEL ver. 0.1j was employed to compare constrained and unconstrained tree topologies using the approximately unbiased, the weighted Shimodaira-Hasegawa, and the weighted Kishino-Hasegawa test (Shimodaira and Hasegawa 2001; Shimodaira 2002, 2008). A *P*-value of < 0.05 was chosen for rejection of the null hypothesis that the constrained and best unconstrained trees are not significantly different.

Network analyses: To visualize all available phylogenetic signals in the 18S rRNA gene alignments, split decomposition analyses were calculated with the computer program SplitsTree ver. 4 (Huson 1998; Huson and Bryant 2006). Since we were interested in the structure of the raw data, phylogenetic networks were generated for each alignment using the neighbornet algorithm with uncorrected distances (Bryant and Moulton 2004). To assess the reliability of the phylogenetic networks, bootstrap analyses with 1000 replicates were carried out.

Analyses of split spectra: A split is a bipartition in a species set, which separates all species of the dataset into two groups (Huson et al. 2010). To find splits present in the ALL and WO alignment and to calculate their support, the computer program SAMS was employed (Wägele and Mayer 2007). This software allows identification of split-supporting nucleotides without reference to a tree and is, therefore, independent of evolutionary model assumptions. Wägele and Rödding (1998) recognized several split-supporting nucleotide positions: binary, asymmetrical, and noisy. Binary positions, i.e., with two character states only, are the most conserved informative positions supporting a clade. Each character state is potentially a plesiomorphy or an apomorphy for a group of a split. Generally, binary positions are rare because substitutions can occur on any branch within a clade, especially in large datasets. Asymmetrical positions support one partition of a split with only one character state, while the other with more than one state. Noisy split-supporting pattern is based on positions with more than two character states, if a majority state within a group still can be identified.

To visualize the counts of supporting positions and the signal-to-noise ratio in the analyzed datasets, we prepared column charts similar to Lento plots (for details, see Lento et al. 1995; Wägele and Mayer 2007; Wägele et al. 2009). For each split, supporting position numbers of in-group partition are shown above and those of out-group partition below the horizontal axis. In addition, three different types of positions in each support column are discerned by colour: binary positions by red colour, asymmetrical by orange, and noisy by yellow. Splits in conflict with tree topology are in dark blue colour.

Quartet mapping: To assess relationships between litostomatean subclasses, we used the quartet mapping technique as implemented in the program Tree-Puzzle ver. 5.2 (Schmidt et al. 2002). This method allows to partition taxa into four clusters (quartets). We conducted the four-cluster likelihood mapping on the ALL, LBS and WO alignments under the GTR model and parameters estimated with Tree-Puzzle. The analyses consisted of sampling neighbor-joining trees with 20,000 quartets.

Acknowledgements

We are very grateful to three anonymous reviewers for their valuable suggestions and very thoughtful comments. Financial support was provided by the Austrian Science Foundation (FWF project P-20360-B17 to Wilhelm Foissner), the German Research Foundation (DFG grant STO414/3-1 to Thorsten Stoeck), and the Slovak Scientific Grant Agency (VEGA projects 1/0600/11 and 1/0248/13 to Peter Vďačný). This work was supported also by the Slovak Researchand Development Agency under the contract No. APVV-0436-12.

Appendix A. Supplementary data

Supplementary data associated with this article can be found, in the online version, at http://dx.doi.org/10.1016/j.protis.2013.11.001.

References

Bryant D, Moulton V (2004) NeighborNet: an agglomerative algorithm for the construction of planar phylogenetic networks. Mol Biol Evol **21**:255–265

Castresana J (2000) Selection of conserved blocks from multiple alignments for their use in phylogenetic analysis. Mol Biol Evol **17**:540–552

Foissner W (1984) Infraciliatur, Silberliniensystem und Biometrie einiger neuer und wenig bekannter terrestrischer, limnischer und mariner Ciliaten (Protozoa: Ciliophora) aus den Klassen Kinetofragminophora, Colpodea und Polyhymenophora. Stapfia **12**:1–165

Foissner W (1996) Ontogenesis in Ciliated Protozoa, with Emphasis on Stomatogenesis. In Hausmann K, Bradbury PC (eds) Ciliates: Cells as Organisms. Fischer-Verlag, Stuttgart, Jena, New York, pp 95–177

Foissner W (1997) Updating the trachelocercids (Ciliophora, Karyorelictea). IV. Transfer of *Trachelocerca entzi* Kahl, 1927 to the Gymnostomatea as a new genus, *Trachelotractus* gen. n. (Helicoprorodontidae). Acta Protozool **36**:63–74

Foissner W, Foissner I (1988) The fine structure of *Fuscheria terricola* Berger et al., 1983 and a proposed new classification of the subclass Haptoria Corliss, 1974 (Ciliophora, Litostomatea). Arch Protistenkd **135**:213–235

Foissner W, Xu K (2007) Monograph of the Spathidiida (Ciliophora, Haptoria). Vol. I: Protospathidiidae, Arcuospathidiidae, Apertospathulidae. Springer, Dordrecht

Foissner W, Agatha S, Berger H (2002) Soil ciliates (Protozoa, Ciliophora) from Namibia (Southwest Africa) with emphasis on two contrasting environments, the Etosha region and the Namib Desert. Denisia **5**:1–1459

Foissner W, Stoeck T, Agatha S, Dunthorn M (2011) Intraclass evolution and classification of the Colpodea (Ciliophora). J Eukaryot Microbiol **58**:397–415

Gabilondo R, Foissner W (2009) Four new fuscheriid soil ciliates (Ciliophora: Haptorida) from four biogeographic regions. Acta Protozool **48**:1–24

Gao S, Song W, Ma H, Clamp JC, Yi Z, Al-Rasheid KAS, Chen Z, Lin X (2008) Phylogeny of six genera of the subclass Haptoria (Ciliophora, Litostomatea) inferred from sequences of the gene coding for small subunit ribosomal RNA. J Eukaryot Microbiol **55**:562–566

Gao S, Strüder-Kypke MC, Al-Rasheid KAS, Lin X, Song W (2010) Molecular phylogeny of three ambiguous ciliate genera: *Kentrophoros*, *Trachelolophos* and *Trachelotractus* (Alveolata, Ciliophora). Zool Scr **39**:305–313

Grain J (1994) Classe de Litostomatea. In Puytorac P de (ed) Infusoires Ciliés–Systematique. Traité de Zoologie. Vol. II, Fasc. 2. Masson, Paris, pp 267-310

Guindon S, Gascuel O (2003) A simple, fast and accurate method to estimate large phylogenies by maximum-likelihood. Syst Biol **52**:696–704

Hall BG (2011) Phylogenetic Trees Made Easy. A How-To Manual. Fourth ed. Sinauer, Sunderland, MA

Huson DH (1998) SplitsTree: a program for analyzing and visualizing evolutionary data. Bioinformatics **14**:68–73

Huson DH, Bryant D (2006) Application of phylogenetic networks in evolutionary studies. Mol Biol Evol **23**: 254–267

Huson DH, Rupp R, Scornavacca C (2010) Phylogenetic Networks. Concepts, Algorithms and Applications. Cambridge University Press, Cambridge

Jankowski AW (2007) Tip Ciliophora Doflein, 1901 [Phylum Ciliophora Doflein, 1901]. In Alimov AF (ed) Protisty: Rukovodstvo po Zoologii [Protista: Handbook of Zoology]. Nauka, St. Petersburg, pp 415-993.(in Russian with English title translation)

Katoh K, Toh H (2008) Recent developments in the MAFFT multiple sequence alignment program. Briefings Bioinf **9**:286–298

Kück P, Mayer C, Wägele J-W, Misof B (2012) Long branch effects distort maximum likelihood phylogenies in simulations despite selection of the correct model. PLoS ONE 7:e36593 (http://dx.doi.org/10.1371/journal.pone.0036593)

Leipe DD, Oppelt A, Hausmann K, Foissner W (1992) Stomatogenesis in the ditransversal ciliate *Homalozoon vermiculare* (Ciliophora, Rhabdophora). Eur J Protistol **28**:198–213

Lemey P, Salemi M, Vandamme AM (2009) The Phylogenetic Handbook: A Practical Approach to Phylogenetic Analysis and Hypothesis Testing. Second ed. Cambridge University Press, Cambridge

Lento GM, Hickson E, Chambers GK, Penny D (1995) Use of spectral analysis to test hypotheses on the origin of pinnipeds. Mol Biol Evol **12**:28–52

Lipscomb DL, Riordan GP (1990) The ultrastructure of *Chaenea teres* and an analysis of the phylogeny of the haptorid ciliates. J Protozool **37**:287–300

Lipscomb DL, Riordan GP (1992) A reexamination of the ultrastructure of *Didinium nasutum* and a reanalysis of the phylogeny of the haptorid ciliates. J Protozool **39**:110–121

Long H, Song W, Al-Rasheid KA, Gong J (2009) Three marine haptorid ciliates from northern China: *Paraspathidium apofuscum* n. sp., *Trachelotractus entzi* (Kahl, 1927) Foissner, 1997 and *Apotrachelotractus variabilis* Long, Song and Warren, 2009 (Protozoa, Ciliophora). J Nat Hist **43**:1749–1761

Lynn DH (2008) The Ciliated Protozoa. Characterization, Classification and Guide to the Literature. Third ed. Springer, Dordrecht

Miller MA, Holder MT, Vos R, Midford PE, Liebowitz T, Chan L, Hoover P, Warnow T (2009) The CIPRES Portals. Available online at http://www.phylo.org/sub_sections/portal

Morrison DA (2011) An Introduction to Phylogenetic Networks. RJR Productions, Uppsala

Nieselt-Struwe K, von Haeseler A (2001) Quartet-mapping, a generalization of the likelihood-mapping procedure. Mol Biol Evol **18**:1204–1219

Pan H, Gao F, Lin X, Warren A, Song W (2013) Three new *Loxophyllum* species (Ciliophora: Pleurostomatida) from China with a brief review of the marine and brackish *Loxophyllum* species. J Eukaryot Microbiol **60**:44–56

Pan H, Gao F, Li J, Lin X, Al-Farraj SA, Al-Rasheid KAS (2010) Morphology and phylogeny of two new pleurostomatid ciliates, *Epiphyllum shenzhenense* n. sp. and *Loxophyllum spirellum* n. sp. (Protozoa, Ciliophora) from a mangrove wetland, South China. J Eukaryot Microbiol **57**: 421–428

Posada D (2008) JModelTest: phylogenetic model averaging. Mol Biol Evol **25**:1253–1256

Ronquist F, Huelsenbeck JP (2003) MrBayes 3: Bayesian phylogenetic inference under mixed models. Bioinformatics **19**:1572–1574

Schmidt HA, Strimmer K, Vingron M, von Haeseler A (2002) TREE-PUZZLE: maximum likelihood phylogenetic analysis using quartets and parallel computing. Bioinformatics **18**:502–504

Shimodaira H (2002) An approximately unbiased test of phylogenetic tree selection. Syst Biol **51**:492–508

Shimodaira H (2008) Testing regions with non-smooth boundaries via multiscale bootstrap. J Stat Plan Infer **138**:1227–1241

Shimodaira H, Hasegawa M (2001) CONSEL: for assessing the confidence of phylogenetic tree selection. Bioinformatics **17**:1246–1247

Stamatakis A, Hoover P, Rougemont J (2008) A rapid bootstrap algorithm for the RAxML web-servers. Syst Biol **75**:758–771

Strüder-Kypke MC, Wright A-DG, Foissner W, Chatzinotas A, Lynn DH (2006) Molecular phylogeny of litostome ciliates (Ciliophora, Litostomatea) with emphasis on free-living haptorian genera. Protist **157**:261–278

Strüder-Kypke MC, Kornilova OA, Lynn DH (2007) Phylogeny of trichostome ciliates (Ciliophora, Litostomatea) endosymbiotic in the Yakut horse (*Equus caballus*). Eur J Protistol **43**:319–328

Swofford DL (2003) PAUP*. Phylogenetic Analysis Using Parsimony (*And Other Methods). Version 4.0b 10. Sinauer, Sunderland, MA

Talavera G, Castresana J (2007) Improvement of phylogenies after removing divergent and ambiguously aligned blocks from protein sequence alignments. Syst Biol **56**:564–577

Vďačný P, Foissner W (2012) Monograph of the dileptids (Protista, Ciliophora, Rhynchostomatia). Denisia **31**:1–529

Vďačný P, Foissner W (2013) Synergistic effects of combining morphological and molecular data in resolving the phylogenetic position of *Semispathidium* (Ciliophora, Haptoria), with description of *S. breviarmatum* sp. n. from tropical Africa. Zool Scr **42**:529–549

Vďačný P, Orsi W, Foissner W (2010) Molecular and morphological evidence for a sister group relationship of the classes Armophorea and Litostomatea (Ciliophora, Intramacronucleata, Lamellicorticata infraphyl. nov.), with an account on basal haptorid litostomateans. Eur J Protistol **46**: 298–309

Vďačný P, Bourland WA, Orsi W, Epstein SS, Foissner W (2011a) Phylogeny and classification of the Litostomatea (Protista, Ciliophora), with emphasis on free-living taxa and the 18S rRNA gene. Mol Phylogenet Evol **59**:510–522

Vďačný P, Orsi W, Bourland WA, Shimano S, Epstein SS, Foissner W (2011b) Morphological and molecular phylogeny of dileptids: resolution at the base of the class Litostomatea (Ciliophora, Intramacronucleata). Eur J Protistol **47**:295–313

Vďačný P, Bourland WA, Orsi W, Epstein SS, Foissner W (2012) Genealogical analyses of multiple loci of litostomatean ciliates (Protista, Ciliophora, Litostomatea). Mol Phylogenet Evol **65**:397–411

Wägele JW, Mayer C (2007) Visualizing differences in phylogenetic information content of alignments and distinction of three classes of long-branch effects. BMC Evol Biol **7**:147 (doi:10.1186/1471-2148-7-147)

Wägele JW, Rödding F (1998) A priori estimation of phylogenetic information conserved in aligned sequences. Mol Phylogenet Evol **9**:358–365

Wägele JW, Letsch H, Klussmann-Kolb A, Mayer C, Misof B, Wägele H (2009) Phylogenetic support values are not necessarily informative: the case of the Serialia hypothesis (a mollusk phylogeny). Front Zool **6**:12 (http://dx.doi.org/10.1186/1742-9994-6-12)

Zhang Q, Simpson A, Song W (2012) Insights into the phylogeny of systematically controversial haptorian ciliates (Ciliophora, Litostomatea) based on multigene analyses. Proc R Soc-B **279**:2625–2635